2D Materials

PURPOSE-LED PUBLISHING™

Proximity Effects, Topological States, and Correlated Physics in Graphene Heterostructures

To cite this article before publication: Klaus Zollner *et al* 2024 *2D Mater.* in press https://doi.org/10.1088/2053-1583/ad9dfd

Proximity Effects, Topological States, and Correlated Physics in Graphene heterostructures

Klaus Zollner‡

Institute for Theoretical Physics, University of Regensburg, 93053 Regensburg, Germany

E-mail: klaus.zollner@physik.uni-regensburg.de

Jaroslav Fabian

Institute for Theoretical Physics, University of Regensburg, 93053 Regensburg, Germany

E-mail: jaroslav.fabian@physik.uni-regensburg.de

Abstract. Graphene spintronics is an emerging field of research that explores the use of graphene's extraordinary spin and charge transport properties to manipulate and control the electron spin degree of freedom for potential applications in information processing and data storage. Particularly interesting are graphene-based van-der-Waals heterostructures, which allow the creation of tailored spintronic properties, emerging from proximity effects, without destroying the unique Dirac states. The possibility to induce customized spin-orbit and exchange coupling in graphene, via band structure engineering, can lead to topologically protected edge states for dissipationless electronics and spintronics. In flat-band graphene materials, in particular, magic-angle bilayer graphene and rhombohedral (ABC stacked) trilayer graphene, the coupling between spin and valley (orbital) degrees of freedom can be coupled by strong Coulomb interactions, leading to a variety of fascinating correlated and superconducting phases. The emerging isospin electronics, combining both the electron spin and valley flavors, can transform the landscape of low-temperature electronics and lead to novel functionalities based on quantum matter. This Perspective explores the latest advancements in proximity effects, topological states, and correlated physics in graphene-based van der Waals heterostructures, discussing the fundamentals for potential applications.

‡ Author to whom any correspondence should be addressed

1. Introduction

Since the discovery of graphene, there has been tremendous interest in utilizing it for spintronics devices due to the extraordinary spin and charge transport properties of the Dirac electrons, with theoretically predicted spin lifetimes of up to microseconds and micrometer spin diffusion lengths [1, 2, 3, 4]. After developing comprehensive technological expertise during the last two decades, graphene devices have started to approach this theory ideal. The key ingredient is protecting graphene from degradation in the ambient environment encapsulating it within isolating hBN layers. This leads to ultraclean and sharp interfaces at the nanoscale, and spin lifetimes reaching 10 ns [2, 5, 6].

Spintronics aims at gaining control over the spin degree of freedom, which is challenging in graphene due to its weak intrinsic spin-orbit coupling (SOC) [7, 8, 9]. In recent years, several efforts concentrated on making graphene "spin active" [10]. To achieve this, graphene was combined with other 2D materials to significantly modify the Dirac states via short-ranged proximity-induced spin interactions [10, 11]. The most prominent examples are transition-metal dichalcogenides (TMDs), which are layered semiconductors that, in addition to being rather stable in air, feature extraordinary optical properties (due to the robust exciton binding), strong SOC especially in the valence bands, and spin-valley locking enabled by the lack of inversion but the presence of in-plane mirror symmetries [12, 13]. Within a graphene/TMD heterostructure, the electronic wavefunctions of the two materials overlap at the interface, leading to what is termed the *proximity spin-orbit* effect: the strong SOC of TMD bands is partially "transferred" into graphene. This is manifested as a spin-orbit splitting of the low energy Dirac bands [14, 15]. Similarly, when graphene is combined with a 2D magnetic semiconductor (such as $Cr_2Ge_2Te_6$ or CrI_3), the Dirac states experience *proximity spin exchange* splitting, which is comparable to the Zeeman splitting due to an external magnetic field [16]. The proximity spin-orbit and spin exchange effects exemplify the power of van der Waals stacking and band structure engineering.

In recent years, the 2D material playground has greatly expanded, offering now a plethora of combination possibilities [17, 18]. By designing multilayer graphene-based heterostructures, with custom-made proximity-induced spin interactions, novel pseudohelical and chiral edge states may appear [19, 20], with potential applications in dissipationless electronics and spintronics. Beyond that, the relative twist angle between the layers is becoming a crucial parameter to tailor proximity spin interactions [21, 22, 23, 24, 25]. Finally, flat-band engineering of graphene structures allows for a variety of correlated phases, such as Stoner isospin magnets, intervalley coherence states, or possibly unconventional superconducting pairing, to be observed [26, 27, 28, 29, 30, 31]. Also here, proximity spin-orbit coupling seems to be highly relevant, for example for stabilizing superconductivity [32, 33] and for generating novel spin-valley couplings [34].

In this perspective, we discuss and elaborate on proximity effects, their tunability knobs, as well as on the emergence of topological states and correlated phases in graphene-based heterostructures. We discuss current theoretical and experimental work and potential device applications. Finally, we provide an outlook on van-der-Waals engineering beyond the currently considered graphene-based heterostructures.

2. Low Energy Physics of (Multilayer) Graphene

We begin by briefly reviewing the intrinsic and extrinsic spin-orbit effects in graphene materials. Monolayer graphene consists of carbon atoms that are arranged in a honeycomb lattice which comprises a triangular Bravais lattice with a two-fold atomic basis in the unit cell [35]. The reciprocal space also consists of a hexagonal Brillouin zone with two nonequivalent valleys K and K′ at the corners. The electronic band structure of graphene near the Fermi level can be described by linearly dispersing Dirac bands located at the Dirac points (K and K′ valleys). The Bloch states of the Dirac bands are almost exclusively formed by p_z-orbitals and are relevant for the unique transport properties. Additionally, a tiny spectral gap of tens of μeV is present, see Fig. 1(a), which is due to the *intrinsic* SOC that lifts the orbital degeneracy; the magnitude of this SOC splitting derives from the SOC of nominally unoccupied d-orbitals which hybridize with the Dirac p_z electrons [7].

When graphene is subject to a transverse (to the carbon sheet) electric field, inversion symmetry gets broken, and the *extrinsic* Rashba SOC appears, lifting the remaining spin degeneracy of the bands. Similarly, when graphene is placed on a substrate, a built-in field across the interface as well as the hybridization across the van der Waals gap can generate the Rashba field by sublattice and inversion symmetry breaking. However, proximity-induced phenomena also modify the intrinsic SOC, leading to topologically distinct low-energy bands depending on the substrate and the stacking, as discussed below.

Naturally occurring (Bernal) bilayer graphene consists of AB-stacked graphene layers, with four atoms in the unit cell. As for the monolayer, the interesting physics happens at the K and K′ valleys. The electronic band structure of bilayer graphene derives from that of single-layer graphene, taking into account the interlayer coupling [36]. In effect, this leads to parabolic bands that touch near the Fermi level at the Dirac points. The layered structure offers a new functionality: layer polarization of low energy bands. Indeed, the low-energy bands are formed by the orbitals of non-dimer atoms of the two layers. A transverse electric field introduces a potential asymmetry in the layers and therefore a band gap opens, see Fig. 1(b). Recent experiments could demonstrate ultraclean gate-tunable band gaps in hBN-encapsulated bilayer graphene of up to 120 meV [5].

Bilayer graphene is thus predestined for gate-defined quantum dots [37, 38] and spin qubits [39, 37]. In addition, bilayer graphene has recently attracted a lot of attention, due to its correlated physics [26, 30, 32], which we address in more detail below. Regarding the spin proximity effects, in bilayer graphene we have the unique situation that the layers can be individually proximitized due to the short-rangeness of proximity effects combined. Combining proximity-induced spin interactions with the layer polarization of the low energy bands allows to swap the spin interactions fully electrically [40, 41].

Placing one more layer, we build trilayer graphene, which comes in different stackings [42]. Perhaps the most intriguing is rhombohedral trilayer graphene with an ABC stacking sequence (predicted to be the most stable one [43]), having similar low energy physics as AB bilayer graphene. In fact, the low energy bands are also formed by non-dimer atoms of the outermost layers, leading to a gate-tunable band gap, see Fig. 1(c). The bands feature a cone-like touching point away from the K point, extending into flat bands near K. Remarkably, correlation physics has been observed in ABC trilayer graphene [44, 45], due to the flat low-energy bands near the

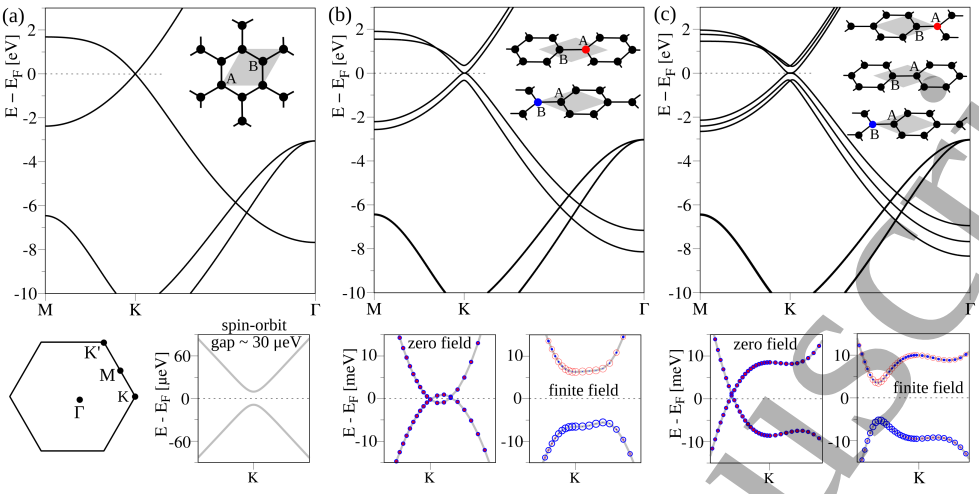

Figure 1. Band structures, geometries, and low energy dispersions of mono-, bi-, and trilayer graphene. (a) Band structure of monolayer graphene. The inset sketches the crystal structure, where the grey rhombus indicates the unit cell with sublattices A and B. Below the band structure, we show the Brillouin zone with relevant high-symmetry points. In addition, a zoom-in on the low energy dispersion near K is shown, displaying the small spin-orbit gap. (b) The same as (a), but for Bernal bilayer graphene. The low energy bands are formed by the non-dimer atoms, indicated by red and blue spheres in the crystal structure, as well as projections in the dispersion. Applying an external electric field opens a band gap and activates the layer polarization of the low-energy bands. (c) The same as (b), but for ABC trilayer graphene. The low-energy bands are formed by the orbitals of the non-dimer atoms from the two outer layers, as indicated. The layer polarization can be induced by a gating field, similar to bilayer graphene.

Fermi level, associated with van Hove singularities in the density of states.

3. Proximity Effects in Graphene Heterostructures

When different materials form van der Waals heterostructures, their wavefunctions weakly hybridize, leading to proximity effects. Graphene, lacking intrinsic SOC and magnetism, is a prime candidate for these effects, as its low-energy p_z orbitals readily hybridize with those of adjacent layers. In the following, we introduce the Hamiltonian of Dirac electrons in proximitized graphene, which provides an effective description for low-energy physics. In addition, we review recent literature results that have demonstrated different proximity effects in graphene-based structures.

3.1. Emergent Hamiltonian of proximitized Graphene

The low-energy bands of spin-orbit and exchange proximitized graphene in the vicinity of the charge-neutrality point (Dirac point) can be modeled with the effective

Hamiltonian considering p_z orbitals only [46]

$$
\begin{aligned}
H &= H_{\rm orb} + H_{\rm so} + H_{\rm ex}, && (1)\\
H_{\rm orb} &= \hbar v_{\rm F}(\kappa\sigma_x k_x + \sigma_y k_y) + \Delta\,\sigma_z, && (2)\\
H_{\rm so} &= \lambda_{\rm KM}\kappa\sigma_z s_z + \lambda_{\rm VZ}\kappa\sigma_0 s_z && (3)\\
&\quad + \lambda_{\rm R}{\rm e}^{-{\rm i}\phi_{\rm R}s_z/2}(\kappa\sigma_x s_y + \sigma_y s_x){\rm e}^{{\rm i}\phi_{\rm R}s_z/2},\\
H_{\rm ex} &= \lambda_{\rm F}\sigma_0 s_z + \lambda_{\rm AF}\sigma_z s_z. && (4)
\end{aligned}
$$

The Hamiltonian, H, has orbital, spin-orbital, and spin exchange parts. The orbital part, $H_{\rm orb}$, describes gapped Dirac states, where $v_{\rm F}$ is the Fermi velocity of Dirac electrons, Δ is the staggered potential (gap), σ are the pseudospin Pauli matrices operating on the sublattice A and B space, and k_x and k_y are the Cartesian components of the electron wave vector measured from K (K′), which parameter $\kappa = 1\,(-1)$ for K (K′). The spin-orbit Hamiltonian $H_{\rm so}$ consists of a Kane-Mele (KM), a valley-Zeeman (VZ), and a Rashba (R) term. The Kane-Mele term is also called intrinsic SOC, as this was one of the initial terms only [47]. However, Dirac states in graphene on 2D spin-orbit material substrates are mostly valley-Zeeman like. Only recently, the Rashba SOC term [47, 48] has been extended to the more general form that obeys time reversal and threefold rotation C_3 symmetries [21, 22]. The Rashba angle $\phi_{\rm R}$ represents a sum of the geometric angle and the quantum phase [49]. The exchange Hamiltonian $H_{\rm ex}$ consists of ferro- and antiferromagnetic terms. The ferromagnetic (F) term describes a uniform effective exchange field from a magnetic substrate, similar to an external magnetic field that leads to a Zeeman splitting. The antiferromagnetic (AF) term describes the non-uniformity of the exchange field that the graphene sublattices experience. Depending on the surrounding materials, very different band structure topologies can arise [10], see Fig. 2. The extension of the model to proximitized multilayer graphene systems is straighforward [42, 41]. Since the proximity effects are short-ranged and limited to neighboring layers, it is sufficient to consider only those layers as affected.

Given a Hamiltonian for a specific class of systems, in this case graphene-based heterostructures, the analysis process to extract the proximity-induced model parameters from ab-initio calculations is as follows. Calculate the proximitized low energy Dirac bands in the vicinity of the K/K' points, including spin and sublattice expectation values, as well as the layer-resolved density of states. One typically finds a small (1-10%) contribution from the surrounding layers in the Dirac bands, which are usually formed by C p_z-orbitals only. To extract the model parameters from the first-principles data, one can employ a least-squares routine [50], taking into account band energies, splittings, and spin and sublattice expectation values. In experiments, the route is different, as the low energy dispersion is typically not directly accessible. However, based on the above model Hamiltonian, several quantities can be calculated or simulated and compared to experiments, such as Hanle spin relaxation [51, 52], weak antilocalization [53, 54], transverse magnetic focusing [55], and Landau-Level spectroscopy [56].

3.2. Spin-Orbit Coupling

Perhaps the most natural way to induce SOC in graphene (while preserving the orbital character of the Dirac cones) is to place it next to an insulator or semiconductor with strong SOC. Metals would also induce strong spin interactions, but the Dirac states would be buried within the conduction bands of the proximitizing material.

One of the first theoretical investigations, considering a graphene/MoS_2 bilayer, found that the Dirac states of graphene are nicely preserved within the TMD band gap [14]. Zooming in on the low energy bands at the Fermi level revealed that the Dirac states are split on the order of 1 meV, see Fig. 2(a), which is giant compared to the $\sim$ 10 μeV intrinsic SOC of graphene [7]. This *induced* splitting stems from the proximity coupling of the monolayers, i. e., the wavefunctions hybridize across the van der Waals gap, such that both layers acquire properties of the other material. In particular, TMDs consist of heavy atoms with large SOC, and the band structure shows sizable spin splittings ($\sim$ 100 meV in the valence bands). This SOC is partially transferred to the p_z orbitals of graphene. Analyzing the Dirac bands wavefunctions in close vicinity of the charge neutrality point within such a heterostructure, one finds that only about 1% of TMD states contribute, which is responsible for the meV-scale splitting. Remarkably, the induced SOC is of valley-Zeeman type, stemming from the spin-valley locking of the TMD, and not of Kane-Mele type as in pristine graphene. Additionally, a Rashba SOC emerges due to inversion symmetry breaking in the heterostructure. The valley-Zeeman SOC is often called Ising SOC and refers to a splitting of the graphene Dirac states at K, as if an external magnetic field would be present, leading to a Zeeman-like band splitting. Due to time-reversal symmetry, the Dirac states at K' are energetically the same, but have the opposite spin. Hence, the charge carriers effectively experience the opposite magnetic field, i. e., a valley-dependent Zeeman-like spin splitting arises.

By employing different TMDs, one can readily change the magnitude of proximity SOC, see Fig. 2(a,b). Eventually, when the spin-orbit splittings exceed the orbital gap, one can tune the Dirac bands into an inverted regime, as for the case of graphene/WSe_2 [57, 58]. With controlled alloying of the TMD, one can even continuously tune the transition from normal to inverted Dirac bands [59]. Due to the short-rangeness of proximity effects, it is typically enough to consider monolayers in theory. However, band offsets and internal electric fields saturate in the few-layer limit [60]. Further tunability knobs for proximity SOC in graphene/TMD heterostructures are the twist angle and gating [24, 61, 25, 62], allowing to tailor the valley-Zeeman and Rashba SOC. Experimental signatures of proximity SOC in graphene are giant spin relaxation anisotropy (spin pointing out of the plane survives 10-100 longer than in-plane spins) [63, 64, 65, 66, 67, 68], the appearance of (unconventional) spin-charge conversion [69, 25, 62, 70, 71, 58, 72], and weak anti-localization [15, 68].

Similarly, other spin-orbit materials have also been considered to induce SOC in graphene. In particular 3D topological insulators such as Bi_2Se_3, Bi_2Te_3, and Sb_2Te_3 can induce sizable SOC in graphene [73, 74, 75, 76] on the order of few meV, tunable by alloying [60, 77] and the twist angle [78]. More recently, also ferroelectric SnTe was considered, predicting giant and anisotropic spin-orbit splittings of Dirac bands [79].

3.3. Exchange Coupling

Magnetism in (nominally nonmagnetic) graphene can be induced by proximity exchange coupling with a ferro- or antiferromagnet. As a consequence, the Dirac bands of graphene will split as if an external magnetic field were present. In contrast to SOC, exchange coupling breaks time-reversal symmetry. Initial studies concentrated on magnetic tunnel junctions, such as graphene/hBN/Co, which are still frequently employed for electrical spin injection [52, 82, 83]. It turns out that the hBN tunnel

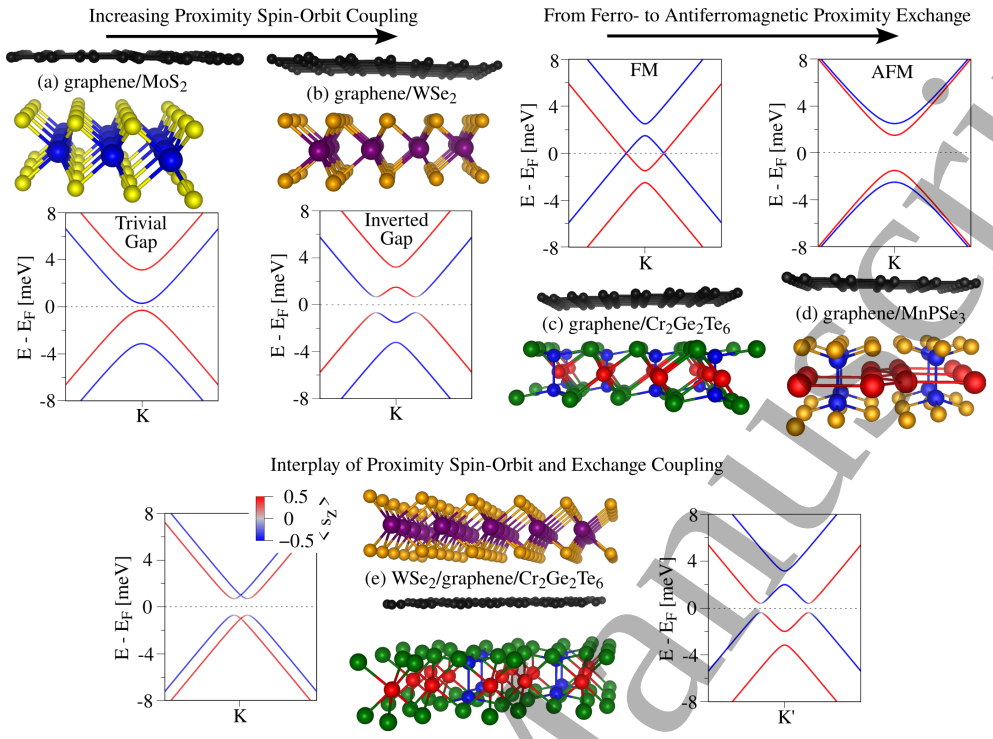

Figure 2. Band structure topologies of proximitized graphene. Presented are exemplary graphene-based van der Waals heterostructures and their model band structures, employing the Hamiltonian Eq. (1), together with realistic parameters from Refs. [57, 23, 80, 81]. The color of the bands represents the spin-z expectation value. (a, b) MoS_2 and WSe_2 provide different proximity-induced SOC of Rashba and valley-Zeeman types. For MoS_2 (WSe_2) the Dirac states exhibit a trivial (inverted) gap. Proximity SOC preserves time-reversal symmetry. (c, d) $Cr_2Ge_2Te_6$ ($MnPSe_3$) provides ferromagnetic = FM (antiferromagnetic = AFM) proximity-induced exchange coupling. Proximity exchange breaks time-reversal symmetry. (e) Doubly proximitized graphene displays both proximity spin interactions. The interplay of proximity SOC and exchange breaks the valley degeneracy of Dirac bands. The low energy bands at K/K' valleys are notably different.

barrier shields the Dirac bands from strong hybridization with the metallic orbitals, but still allows some amount of exchange coupling to be transferred to the p_z orbitals of graphene [84]. Other earlier sources for proximity exchange in graphene were EuO, EuS, and Yttrium-Iron-Garnet [85, 86, 87, 88], having either poor interface quality or low Curie temperature to make a stronger impact.

Despite the success of the aforementioned tunnel spin injection geometries, layered 2D magnets provide a viable alternative to induce exchange splitting for Dirac electrons, see Fig. 2(c,d). Of particular interest are magnetic insulators or semiconductors such as $Cr_2Ge_2Te_6$ [81, 89, 16], CrI_3 [90, 91, 92, 93], or $MnPSe_3$ [20, 80], which can modulate the band structure of graphene (or another nonmagnetic material) without significant charge transfer and without contributing additional transport channels. Remarkably, ferromagnetic and antiferromagnetic proximity-induced exchange coupling can be realized by 2D magnets, see Fig. 2(c,d). The

only drawback for device applications is the Curie and Neel temperatures of those 2D magnets, as they are well below ambient conditions. Fortunately, there are already metallic 2D magnets available, operating at room temperature, which are long-sought building blocks for next-generation low-power magnetoelectronic and spintronic devices [94, 95]. It is perhaps only a matter of time until air-stable 2D magnetic insulators are synthesized, providing room-temperature platforms for "magnetizing" graphene.

Proximity exchange effects in graphene can be observed by quantum anomalous Hall effect [96], magnetoresistance [97], or nonlocal spin transport experiments [87]. Remarkably, recent studies have demonstrated spin injection and the giant electrostatic control of spin polarization in exchange proximitized graphene on antiferromagnetic CrSBr [98, 99]. These results are promising for the development of gate-controllable spin valves and spin filters.

3.4. Proximity induced superconductivity

Proximity effects in condensed matter stem from superconductivity. In a junction formed by a normal metal and a superconductor, the Cooper pairs from the superconductor can penetrate, within the coherence length, into the metal. Vice versa, the superconducting pairing is somewhat reduced by the contact with the normal conductor. The most spectacular demonstration of the superconducting proximity is the Josephson effect, in which the superconducting pairing persists through a barrier (normal metal or insulator) connecting two superconducting electrodes.

While monolayer graphene does not appear to support Cooper pairs at experimentally accessible temperatures, superconductivity can be induced by the proximity effect. Experiments to detect the proximity superconductivity include gate-tunable supercurrent in graphene with Ti/Al contacts [100], ballistic Josephson effect [101] and supercurrent in the quantum Hall regime [102] in graphene with MoRe edge contacts, and Andreev reflection at the interface of superconducting-graphene/normal-graphene in graphene/$NbSe_2$ heterostructures [103].

The advantage of 2D superconductors, for proximitizing graphene, lies again in the bond-free and atomically-sharp van der Waals interface. Remarkably, theoretical predictions report on twist-tunable proximity-induced superconductivity in graphene/$NbSe_2$ [104], which is in line with recent experiments [103]. Furthermore, since $NbSe_2$ is a TMD with large SOC, the twist-tunability of proximity-induced SOC has been recently considered in graphene/$NbSe_2$ [105]. In addition, $NbSe_2$ exhibits a charge density wave phase that can be imprinted in graphene [106]. This demonstrates the complex interplay of several proximity effects in graphene/$NbSe_2$ van der Waals heterostructures, which is a potential playground to host chiral Majorana fermions [107]. Remarkably, graphene superconductivity emerges beyond monolayers, as discussed below.

3.5. Interplay of Proximity Effects

When graphene is encapsulated, one can either enhance or weaken proximity-induced phenomena. For example, when graphene is encapsulated by TMD layers, their relative twist angle tunes the interference of proximity-induced SOC [49, 24]. Similarly, when graphene is encapsulated by 2D magnets, their relative magnetizations and twist angles can be used to tailor the proximity-induced exchange coupling [41, 23].

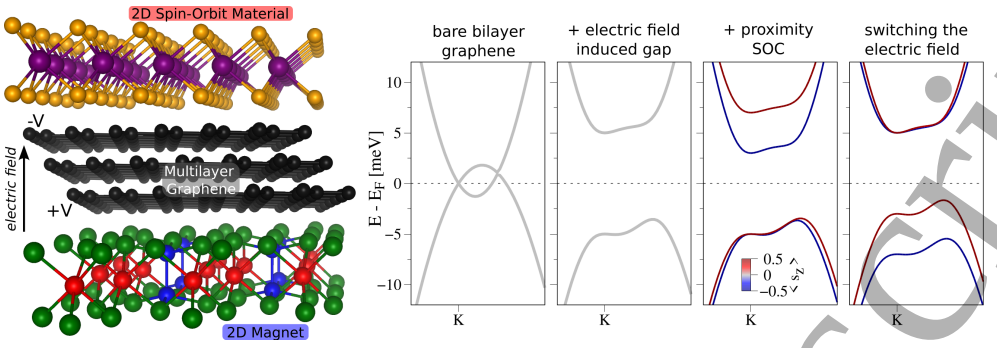

Figure 3. Left: Schematics of proximity physics in encapsulated multilayer graphene heterostructures. In multilayer graphene, only the outer layers are subject to short-range proximity effects, stemming from 2D spin-orbit materials or magnets. An external electric field is employed to tune the potentials ($\pm$V) of the outermost graphene layers. Together with the layer polarization of the low energy bands, see Fig. 1, proximity spin splittings can be swapped from valence to conduction band. Right: We show exemplary low energy model band structures for bare bilayer graphene without and with electric field, as well as the switching of proximity SOC from conduction to valence bands in WSe_2/bilayer-graphene. The physics of differently proximitized bi- and trilayer graphene structures are explained in more detail in Refs. [108, 109, 40, 42, 41].

The story becomes more complicated when different materials are employed for encapsulation. For example, when graphene is doubly proximitized by a TMD and a 2D magnet, see Fig. 2(e), the two spin interactions, spin-orbit and exchange coupling, interfere with each other, break the valley degeneracy, and serve as a playground for gate-tunable spin-orbit torque [81], topological phases [20], spin qubits [110], and correlated phases [111, 34]. In proximitized bi- and trilayer graphene, spin interactions can be turned on and off, see Fig. 3, or even swapped fully electrically due to the additional layer polarization [40, 41, 42, 108, 109], allowing for spin valve and filter operations.

As already mentioned, certain 2D materials can induce multiple proximity effects at the same time. One example are graphene/$NbSe_2$ heterostructures, where SOC [105], superconductivity [104], and a charge density wave phase [106] have been imprinted to graphene by proximity. Recently, also graphene/TaS_2 heterostructures have been investigated, simultaneously showing spin-orbit, exchange, and charge density wave proximity effects [112]. The only requirement to induce multiple proximity effects simultaneously is that the substrate hosts multiple spin interactions, such as magnetic topological insulators $MnBi_2Te_4$ [113], topological superconductors $FeTe_{1-x}Se_x$ [114], or magnetic TMDs [115].

4. Emergence of Topological States and Correlated Phases

Since the discovery of correlated physics in magic-angle twisted bilayer graphene [26], there have been numerous studies to understand its origin and the various flavors of correlated states in multilayer graphene systems [27, 29, 116, 117, 118]. In addition, since spin interactions have been induced by the proximity effect in graphene, there is an increasing interest in the design of topological edge states for dissipationless electronics and spintronics [19, 119, 20, 107, 120]. In the following, we further discuss

these two branches of graphene physics.

4.1. Topological States

Topology in graphene dates back to the initial studies of Kane and Mele, which predicted the quantum spin Hall effect due to the spin-orbit gap in pristine graphene [47, 121]. However, in experimentally relevant samples, Rashba coupling, staggered sublattice potential, and other proximity effects arise, typically dominating over the weak intrinsic SOC of tens of μeV. Furthermore, the presence of electron-hole puddles causes significant fluctuations in the Fermi level (10-100 meV), making it difficult to search for topological states within the spin-orbit gap of the intrinsic SOC.

It was soon realized that proximity effects could aid in designing more robust topological states, as they can significantly enhance SOC accompanied by proximity exchange and superconductivity, depending on the substrate [122, 123]. More recent efforts concentrated on providing a unified picture of the topological nature of proximitized graphene and the existence and character of protected edge states [19, 107, 20, 119].

One of the first surprising observations was the fact that the induced SOC, for graphene on various substrates [124, 57, 60, 125], is mostly of valley-Zeeman and Rashba type, and not of Kane-Mele type as in pristine graphene [7, 8]. In fact, Kane-Mele (sublattice even) intrinsic SOC manifests as quantum spin Hall states (QSHS) characterized by nontrivial $\mathcal{Z}_2$ invariant, see Fig. 4, while valley-Zeeman (sublattice-odd) intrinsic SOC manifests as pseudohelical states with $\mathcal{Z}_2 = 0$ [19]. Both of them are robust against (time-reversal) impurity scattering and show helical edge currents in narrow graphene zigzag ribbons, but the pseudohelical states display pseudospin-spin locking contrary to QSHS.

Once magnetic proximity effects are induced in graphene, in addition to proximity SOC, quantum anomalous Hall states (QAHS) can arise [20], which are characterized by Chern number $\mathcal{C}$. Proximity exchange coupling in graphene can be ferromagnetic, antiferromagnetic, or ferrimagnetic [23, 80], while proximity SOC can be of Kane-Mele, valley-Zeeman, and Rashba type [14, 126], providing a broad phase space to potentially observe QAHS with Chern numbers $\mathcal{C} = 1,\ 2$. Finally, when graphene is in the QAHS phase and proximity superconductivity is added, also chiral topological superconductor phases can form [107].

Until now, no clear evidence exists for a QSHS in graphene, even when proximitized. Signatures of QSHS have only been observed in the presence a of very large magnetic field [127]. One of the first more clear demonstrations has been made when graphene is decorated with Bi_2Te_3 nanoparticles, locally enhancing SOC [128]. One of the obstacles, that hinders the observation of topological states in (proximitized) graphene is the size of the topological gap. Even, when proximity effects are at play, the gap is typically small compared to other disturbing factors like the thermal energy and electron-hole puddles [129, 130]. In multilayer graphene structures, it has been reported that topologically protected states have been realized in proximitized bilayer [131] and pentalayer graphene [132].

4.2. Correlated Phases

A prerequisite for the formation of correlated phases in graphene-based structures is van-Hove singularities (peaks in the density of states), corresponding to flat bands

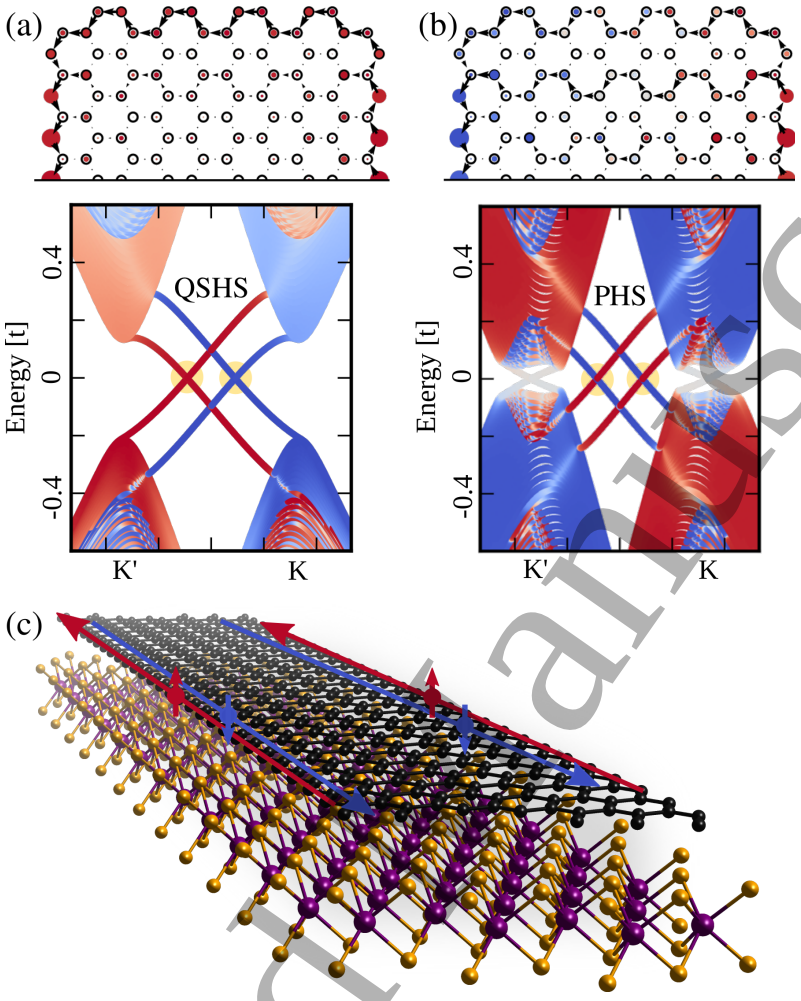

Figure 4. (a) Real space representation of a single quantum spin Hall state (QSHS), localized at the edges, along with the energy spectrum of a zigzag graphene nanoribbon in the presence of Kane-Mele SOC. The color indicates the spin-expectation value (red = spin up, blue = spin down). The relevant states are indicated in the spectrum. (b) The same as (a), but for valley-Zeeman SOC, resulting in pseudo-helical states (PHS), accompanied by a spin-flip at the armchair edges. (c) Sketch of pseudo-helical states in graphene proximitized by a strong spin-orbit material, e.g., WSe_2. Figures (a) and (b) adapted from Ref. [19].

in the electronic dispersion with minimum Fermi velocity, leading to large electron-electron interactions, see Fig. 5. The first demonstration of correlated physics was in magic-angle twisted bilayer graphene (MATBG) in 2018 [26, 133]. For small ($\sim 1^\circ$) twist angles, bilayer graphene exhibits flat bands near zero Fermi energy, resulting in correlated insulator behavior and superconductivity upon different filling factors of the moiré Brillouin zone. Several experimental and theoretical efforts aimed to understand the correlation physics in MATBG [33, 134, 28, 135, 136, 137, 138, 139, 140, 141, 142, 143, 144, 145, 146]. It turned out that a relatively simple real space picture, based on localized heavy fermions at AA stacking regions, combined with delocalized

semimetallic conduction band states, captures the ground state and topological physics very well [147, 27]. This is a prime example of reformulating an initial highly complex problem into a relatively simple model language. Nevertheless, flat bands are already intrinsically present in multilayer graphene systems, such as bernal bilayer graphene and rhombohedral trilayer graphene. Experiments and theory have demonstrated, that also in these systems correlated behavior arises, with [32, 34, 111, 148, 149] and without [30, 31, 44, 45, 150, 151, 152] proximity coupling to other 2D materials. In fact, it appears that the proximity-induced valley-Zeeman SOC, originating from a TMD, even stabilizes superconducting phases in AB and ABC graphene multilayer systems [32, 153, 154, 155, 156].

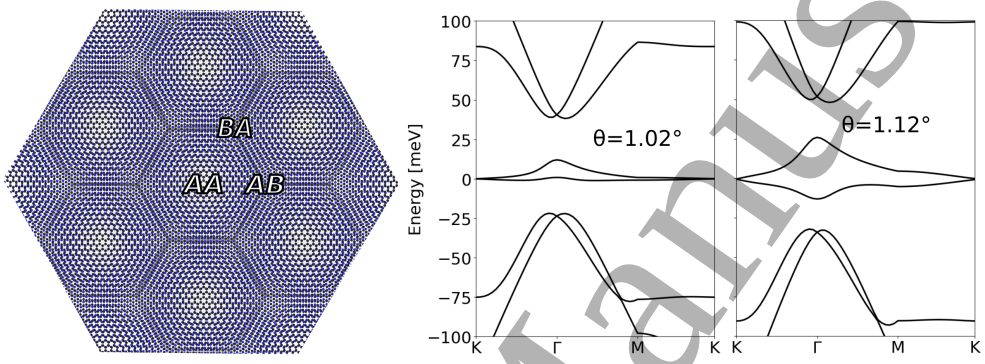

Figure 5. Left: Bilayer graphene twisted at small angles ($\sim 1°$) shows a long range moiré pattern. Lattice relaxation plays an important role in the formation of localized states at AA stacking regions [146]. Middle: The low energy dispersion at $\theta = 1.02°$, calculated from an exact continuum model [145], features flat bands near zero Fermi energy, being well separated from dispersive bands at higher energies. Right: By small twist angle deviations ($\sim 0.1°$) from the 'magic' angle, the low energy bands recover their dispersiveness and correlated behavior gets quenched.

5. Perspectives and Challenges for Theory and Experiment

Proximity effects in 2D materials have by now been firmly established. Aided by structural engineering—stacking, twisting, straining—as well as gating and doping, proximity effects can effectively alter the spin, magnetic, and superconducting properties of 2D materials. Given the vast choices of layered materials [17, 18], including strong spin-orbit materials, magnets, superconductors, ferroelectric, and topological materials, it is not surprising that we still know very little about their various combinations.

For theory, one challenge is to develop realistic models for proximity effects which necessarily involve large supercells, strained to generate commensurate structures. Strain can cause problems in determining accurate proximity parameters, but also stacking. Furthermore, the effective Hamiltonians describing the proximity effects are useful for making qualitative predictions, but it is not clear how far one can push them in describing experimental structures. For example, a van der Waals stack contains a spatially varying registry of atoms, each atom feeling a different environment from the proximitizing material. It is expected that the proximity effects will then result in a spatially non-uniform pattern, so that spin-orbit and exchange couplings should

vary throughout the lattice. Determination of such a pattern, both theoretically and experimentally, would certainly be highly valuable.

In fact, graphene-based van der Waals heterostructures have already opened new avenues for many scientific and technological advances in spintronic devices, such as tunnel junctions [157, 158], optospintronics devices [159, 14, 160, 10], spin-logic devices [161], spin transistors [108], and spin-orbit torque magnetic random access memories [162, 163, 164, 165, 166, 167]. All these technologies rely on the proximity coupling of the layers. Another challenge lies in predicting material combinations that optimize specific functionalities. For instance, large tunneling magnetoresistance requires compatible Bloch states between tunneling electrons and barrier conduction states. A systematic understanding of such material characteristics is still lacking. Moreover, while theoretical predictions have been made for spin-orbit engineering involving TMDs and topological insulators (discussed in the main text), experimental verification, particularly for the vanishing valley-Zeeman coupling at 30° twist angle in graphene/TMD heterostructures, remains elusive. We anticipate that high-throughput AI tools will prove valuable in future spin-orbit engineering and the discovery of optimal material combinations for spin-dependent tunneling.

After an initial period of slow progress, researchers are now reporting significant advancements in the experimental realization of spin-orbit torques [162, 163, 164, 165, 166, 167]. Given their immense technological relevance, there is a strong push to achieve efficient magnetization switching by passing a current through the heterostructure. Many questions remain open. How fast could the switching be? Can it be controlled by gating? What is the magnetization damping coefficient? For theory and experiment, it is important to find out what is the relevant mechanism of the torque. Is the spin accumulation coming from the charge-to-spin conversion or is it the proximity spin-orbit exchange in the magnet from a strong SOC material? Such questions are relevant, since in ultrathin samples it is not expected that transverse (to the sheets) spin Hall currents would flow, enabling the torque. Also, it is not obvious what is the role of defects in providing the necessary damping torque.

Twist angle is a great tool in designing new functional materials. In magnets, twisted heterostructures could give us platforms for topological magnetic excitations (skyrmions), and modulate the magneto tunneling effects, as in a recent experiment [168, 169]. It is also not yet experimentally confirmed that twisting can profoundly change the proximity effect (say, flip the proximity spin polarization).

Correlated phases pose perhaps most challenges, but also perspectives. The origin of superconducting pairing is an outstanding puzzle, and the question if SOC can stabilize superconductivity is still open. New possibilities for spintronics arise from the possibility of isospin (spin and valley) engineering. Isospin polarization results in orbital magnetism, which can be manipulated electrically by gating and by electrical currents. To what extent can the isospin be manipulated by external fields similarly to the electron spin being controlled magnetically? Can valley-Zeeman coupling lead to a coherent coupling between the two flavors? Can proximity spin exchange stabilize the triplet component (if present) in graphene superconductors? The potential of isospin manipulation to enable new functionalities is vast and highly anticipated.

Acknowledgments

K. Z. and J. F. acknowledge funding by the Deutsche Forschungsgemeinschaft (DFG, German Research Foundation) SFB 1277 (Project No. 314695032), SPP 2244

(Project No. 443416183), the European Union Horizon 2020 Research and Innovation Program under contract number 881603 (Graphene Flagship) and FLAGERA project 2DSOTECH.

References

[1] Han W, Kawakami R K, Gmitra M and Fabian J 2014 *Nat. Nanotechnol.* **9** 794

[2] Avsar A, Ochoa H, Guinea F, Özyilmaz B, van Wees B J and Vera-Marun I J 2020 *Rev. Mod. Phys.* **92**(2) 021003 URL https://link.aps.org/doi/10.1103/RevModPhys.92.021003

[3] Roche S and Valenzuela S O 2014 *Journal of Physics D: Applied Physics* **47** 094011 URL https://dx.doi.org/10.1088/0022-3727/47/9/094011

[4] Ertler C, Konschuh S, Gmitra M and Fabian J 2009 *Phys. Rev. B* **80**(4) 041405 URL https://link.aps.org/doi/10.1103/PhysRevB.80.041405

[5] Icking E, Banszerus L, Wörtche F, Volmer F, Schmidt P, Steiner C, Engels S, Hesselmann J, Goldsche M, Watanabe K, Taniguchi T, Volk C, Beschoten B and Stampfer C 2022 *Advanced Electronic Materials* **8** 2200510 (*Preprint* https://onlinelibrary.wiley.com/doi/pdf/10.1002/aelm.202200510) URL https://onlinelibrary.wiley.com/doi/abs/10.1002/aelm.202200510

[6] Martini L, Mišeikis V, Esteban D, Azpeitia J, Pezzini S, Paletti P, Ochapski M W, Convertino D, Hernandez M G, Jimenez I and Coletti C 2023 *ACS Applied Materials & Interfaces* **15** 37794–37801

[7] Gmitra M, Konschuh S, Ertler C, Ambrosch-Draxl C and Fabian J 2009 *Phys. Rev. B* **80**(23) 235431

[8] Sichau J, Prada M, Anlauf T, Lyon T J, Bosnjak B, Tiemann L and Blick R H 2019 *Phys. Rev. Lett.* **122**(4) 046403 URL https://link.aps.org/doi/10.1103/PhysRevLett.122.046403

[9] Banszerus L, Frohn B, Fabian T, Somanchi S, Epping A, Müller M, Neumaier D, Watanabe K, Taniguchi T, Libisch F, Beschoten B, Hassler F and Stampfer C 2020 *Phys. Rev. Lett.* **124**(17) 177701 URL https://link.aps.org/doi/10.1103/PhysRevLett.124.177701

[10] Sierra J F, Fabian J, Kawakami R K, Roche S and Valenzuela S O 2021 *Nature Nanotechnology* 1–13

[11] Žutić I, Matos-Abiague A, Scharf B, Dery H and Belashchenko K 2019 *Mater. Today* **22** 85

[12] Xiao D, Liu G B, Feng W, Xu X and Yao W 2012 *Phys. Rev. Lett.* **108** 196802 URL https://link.aps.org/doi/10.1103/PhysRevLett.108.196802

[13] Kormányos A, Burkard G, Gmitra M, Fabian J, Zólyomi V, Drummond N D, Fal'ko V and Fal'ko V 2014 *2D Mater.* **2** 022001

[14] Gmitra M and Fabian J 2015 *Phys. Rev. B* **92**(15) 155403

[15] Fülöp B, Márffy A, Zihlmann S, Gmitra M, Tóvári E, Szentpéteri B, Kedves M, Watanabe K, Taniguchi T, Fabian J *et al.* 2021 *npj 2D Materials and Applications* **5** 82

[16] Karpiak B, Cummings A W, Zollner K, Vila M, Khokhriakov D, Hoque A M, Dankert A, Svedlindh P, Fabian J, Roche S and Dash S P 2019 *2D Mater.* **7** 015026 URL https://iopscience.iop.org/article/10.1088/2053-1583/ab5915

[17] Zhou J, Shen L, Costa M D, Persson K A, Ong S P, Huck P, Lu Y, Ma X, Chen Y, Tang H *et al.* 2019 *Scientific data* **6** 86

[18] Gjerding M N, Taghizadeh A, Rasmussen A, Ali S, Bertoldo F, Deilmann T, Knøsgaard N R, Kruse M, Larsen A H, Manti S, Pedersen T G, Petralanda U, Skovhus T, Svendsen M K, Mortensen J J, Olsen T and Thygesen K S 2021 *2D Materials* **8** 044002 URL https://dx.doi.org/10.1088/2053-1583/ac1059

[19] Frank T, Högl P, Gmitra M, Kochan D and Fabian J 2018 *Phys. Rev. Lett.* **120**(15) 156402

[20] Högl P, Frank T, Zollner K, Kochan D, Gmitra M and Fabian J 2020 *Phys. Rev. Lett.* **124**(13) 136403

[21] David A, Rakyta P, Kormányos A and Burkard G 2019 *Phys. Rev. B* **100**(8) 085412 URL https://link.aps.org/doi/10.1103/PhysRevB.100.085412

[22] Li Y and Koshino M 2019 *Phys. Rev. B* **99**(7) 075438 URL https://link.aps.org/doi/10.1103/PhysRevB.99.075438

[23] Zollner K and Fabian J 2022 *Phys. Rev. Lett.* **128**(10) 106401

[24] Zollner K, João S a M, Nikolić B K and Fabian J 2023 *Phys. Rev. B* **108**(23) 235166 URL https://link.aps.org/doi/10.1103/PhysRevB.108.235166

[25] Yang H, Martín-García B, Kimák J, Schmoranzerová E, Dolan E, Chi Z, Gobbi M, Němec P, Hueso L E and Casanova F 2023 *arXiv:2312.10227*

[26] Cao Y, Fatemi V, Fang S, Watanabe K, Taniguchi T, Kaxiras E and Jarillo-Herrero P

2018 *Nature* **556** 43 URL http://dx.doi.org/10.1038/nature26160http://www.nature.com/articles/nature26160
[27] Bernevig B A and Efetov D K 2024 *Physics Today* **77** 38–44 ISSN 0031-9228 (*Preprint* https://pubs.aip.org/physicstoday/article-pdf/77/4/38/19858215/38_1_pt.jvsd.yhyd.pdf) URL https://doi.org/10.1063/pt.jvsd.yhyd
[28] Lu X, Stepanov P, Yang W, Xie M, Aamir M A, Das I, Urgell C, Watanabe K, Taniguchi T, Zhang G *et al.* 2019 *Nature* **574** 653–657
[29] Shen C, Ledwith P J, Watanabe K, Taniguchi T, Khalaf E, Vishwanath A and Efetov D K 2023 *Nature Materials* **22** 316–321
[30] Seiler A M, Geisenhof F R, Winterer F, Watanabe K, Taniguchi T, Xu T, Zhang F and Weitz R T 2022 *Nature* **608** 298–302
[31] Pantaleón P A, Jimeno-Pozo A, Sainz-Cruz H, Phong V T, Cea T and Guinea F 2023 *Nature Reviews Physics* **5** 304–315
[32] Zhang Y, Polski R, Thomson A, Lantagne-Hurtubise É, Lewandowski C, Zhou H, Watanabe K, Taniguchi T, Alicea J and Nadj-Perge S 2023 *Nature* **613** 268–273
[33] Arora H S, Polski R, Zhang Y, Thomson A, Choi Y, Kim H, Lin Z, Wilson I Z, Xu X, Chu J H *et al.* 2020 *Nature* **583** 379–384
[34] Zhumagulov Y, Kochan D and Fabian J 2024 *Phys. Rev. Lett.* **132**(18) 186401 URL https://link.aps.org/doi/10.1103/PhysRevLett.132.186401
[35] Geim A K and Novoselov K S 2007 *Nat. Mater.* **6** 183
[36] Konschuh S, Gmitra M, Kochan D and Fabian J 2012 *Phys. Rev. B* **85** 115423
[37] Garreis R, Tong C, Terle J, Ruckriegel M J, Gerber J D, Gächter L M, Watanabe K, Taniguchi T, Ihn T, Ensslin K *et al.* 2024 *Nature Physics* 1–7
[38] Banszerus L, Möller S, Hecker K, Icking E, Watanabe K, Taniguchi T, Hassler F, Volk C and Stampfer C 2023 *Nature* **618** 51–56
[39] Denisov A O, Reckova V, Cances S, Ruckriegel M J, Masseroni M, Adam C, Tong C, Gerber J D, Huang W W, Watanabe K, Taniguchi T, Ihn T, Ensslin K and Duprez H 2024 *arXiv:2403.08143*
[40] Zollner K, Gmitra M and Fabian J 2020 *Phys. Rev. Lett.* **125**(19) 196402
[41] Zollner K and Fabian J 2021 *Phys. Rev. B* **104**(7) 075126
[42] Zollner K, Gmitra M and Fabian J 2022 *Phys. Rev. B* **105**(11) 115126 URL https://link.aps.org/doi/10.1103/PhysRevB.105.115126
[43] Guerrero-Avilés R, Pelc M, Geisenhof F R, Weitz R T and Ayuela A 2022 *Nanoscale* **14**(43) 16295–16302 URL http://dx.doi.org/10.1039/D2NR01985J
[44] Zhou H, Xie T, Ghazaryan A, Holder T, Ehrets J R, Spanton E M, Taniguchi T, Watanabe K, Berg E, Serbyn M *et al.* 2021 *Nature* **598** 429–433
[45] Zhou H, Xie T, Taniguchi T, Watanabe K and Young A F 2021 *Nature* **598** 434–438
[46] Kochan D, Irmer S and Fabian J 2017 *Phys. Rev. B* **95**(16) 165415
[47] Kane C L and Mele E J 2005 *Phys. Rev. Lett.* **95** 226801
[48] Bychkov Y A and Rashba E I 1984 *Journal of Physics C: Solid State Physics* **17** 6039
[49] Péterfalvi C G, David A, Rakyta P, Burkard G and Kormányos A 2022 *Physical Review Research* **4** L022049
[50] Newville M, Stensitzki T, Allen D B and Ingargiola A 2014 LMFIT: Non-Linear Least-Square Minimization and Curve-Fitting for Python URL https://doi.org/10.5281/zenodo.11813
[51] Tombros N, Tanabe S, Veligura A, Jozsa C, Popinciuc M, Jonkman H T and van Wees B J 2008 *Phys. Rev. Lett.* **101**(4) 046601
[52] Tombros N, Jozsa C, Popinciuc M, Jonkman H T and van Wees B J 2007 *Nature* **448** 571
[53] Wakamura T, Reale F, Palczynski P, Zhao M Q, Johnson A T C, Guéron S, Mattevi C, Ouerghi A and Bouchiat H 2019 *Phys. Rev. B* **99**(24) 245402 URL https://link.aps.org/doi/10.1103/PhysRevB.99.245402
[54] Garcia J H, Cummings A W and Roche S 2017 *Nano letters* **17** 5078–5083
[55] Rao Q, Kang W H, Xue H, Ye Z, Feng X, Watanabe K, Taniguchi T, Wang N, Liu M H and Ki D K 2023 *Nature communications* **14** 6124
[56] Rao Q, Xue H and Ki D K 2024 *physica status solidi (b)* **261** 2300397 URL https://onlinelibrary.wiley.com/doi/abs/10.1002/pssb.202300397
[57] Gmitra M, Kochan D, Högl P and Fabian J 2016 *Phys. Rev. B* **93**(15) 155104
[58] Herling F, Safeer C K, Ingla-Aynés J, Ontoso N, Hueso L E and Casanova F 2020 *APL Materials* **8** 071103
[59] Khatibi Z and Power S R 2022 *Phys. Rev. B* **106**(12) 125417 URL https://link.aps.org/doi/10.1103/PhysRevB.106.125417
[60] Zollner K and Fabian J 2019 *Phys. Rev. B* **100**(16) 165141

[61] Lee S, de Sousa D J P, Kwon Y K, de Juan F, Chi Z, Casanova F and Low T 2022 *Phys. Rev. B* **106**(16) 165420
[62] Safeer C, Ingla-Aynés J, Herling F, Garcia J H, Vila M, Ontoso N, Calvo M R, Roche S, Hueso L E and Casanova F 2019 *Nano Lett.* **19** 1074
[63] Cummings A W, Garcia J H, Fabian J and Roche S 2017 *Phys. Rev. Lett.* **119**(20) 206601
[64] Ghiasi T S, Ingla-Aynés J, Kaverzin A A and Van Wees B J 2017 *Nano Lett.* **17** 7528
[65] Omar S, Madhushankar B N and van Wees B J 2019 *Phys. Rev. B* **100**(15) 155415 URL https://link.aps.org/doi/10.1103/PhysRevB.100.155415
[66] Garcia J H, Vila M, Cummings A W and Roche S 2018 *Chem. Soc. Rev.* **47** 3359
[67] Omar S and van Wees B J 2017 *Phys. Rev. B* **95**(8) 081404 URL https://link.aps.org/doi/10.1103/PhysRevB.95.081404
[68] Omar S and van Wees B J 2018 *Phys. Rev. B* **97**(4) 045414
[69] Hoque A M, Khokhriakov D, Zollner K, Zhao B, Karpiak B, Fabian J and Dash S P 2021 *Communications Physics* **4** 124
[70] Safeer C, Ontoso N, Ingla-Aynés J, Herling F, Pham V T, Kurzmann A, Ensslin K, Chuvilin A, Robredo I, Vergniory M G *et al.* 2019 *Nano letters* **19** 8758–8766
[71] Safeer C K, Herling F, Choi W Y, Ontoso N, Ingla-Aynés J, Hueso L E and Casanova F 2021 *2D Materials* **9** 015024
[72] Ingla-Aynés J, Groen I, Herling F, Ontoso N, Safeer C K, de Juan F, Hueso L E, Gobbi M and Casanova F 2022 *2D Materials* **9** 045001
[73] Song K, Soriano D, Cummings A W, Robles R, Ordejón P and Roche S 2018 *Nano Lett.* **18** 2033 ISSN 1530-6984 URL https://pubs.acs.org/sharingguidelineshttp://pubs.acs.org/doi/10.1021/acs.nanolett.7b05482
[74] Khokhriakov D, Cummings A W, Song K, Vila M, Karpiak B, Dankert A, Roche S and Dash S P 2018 *Sci. Adv.* **4** eaat9349 URL http://advances.sciencemag.org/lookup/doi/10.1126/sciadv.aat9349
[75] Jafarpisheh S, Cummings A W, Watanabe K, Taniguchi T, Beschoten B and Stampfer C 2018 *Phys. Rev. B* **98** 241402 URL https://link.aps.org/doi/10.1103/PhysRevB.98.241402
[76] Zhang J, Triola C and Rossi E 2014 *Phys. Rev. Lett.* **112**(9) 096802 URL https://link.aps.org/doi/10.1103/PhysRevLett.112.096802
[77] Zollner K and Fabian J 2021 *physica status solidi (b)* **258** 2000081
[78] Naimer T and Fabian J 2023 *Phys. Rev. B* **107**(19) 195144 URL https://link.aps.org/doi/10.1103/PhysRevB.107.195144
[79] Milivojević M, Gmitra M, Kurpas M, Štich I and Fabian J 2024 *arXiv:2402.09045*
[80] Zollner K and Fabian J 2022 *Phys. Rev. B* **106**(3) 035137 URL https://link.aps.org/doi/10.1103/PhysRevB.106.035137
[81] Zollner K, Petrović M D, Dolui K, Plecháč P, Nikolić B K and Fabian J 2020 *Phys. Rev. Research* **2**(4) 043057
[82] Kamalakar M V, Dankert A, Kelly P J and Dash S P 2016 *Sci. Rep.* **6** 21168
[83] Kamalakar M V, Dankert A, Bergsten J, Ive T and Dash S P 2014 *Sci. Rep.* **4** 6146
[84] Zollner K, Gmitra M, Frank T and Fabian J 2016 *Phys. Rev. B* **94**(15) 155441
[85] Hallal A, Ibrahim F, Yang H, Roche S and Chshiev M 2017 *2D Mater.* **4** 025074
[86] Wei P, Lee S, Lemaitre F, Pinel L, Cutaia D, Cha W, Katmis F, Zhu Y, Heiman D, Hone J, Moodera J S and Chen C T 2016 *Nat. Mater.* **15** 711
[87] Leutenantsmeyer J C, Kaverzin A A, Wojtaszek M and van Wees B J 2016 *2D Mater.* **4** 014001
[88] Swartz A G, Odenthal P M, Hao Y, Ruoff R S and Kawakami R K 2012 *ACS Nano* **6** 10063
[89] Zhang J, Zhao B, Yao Y and Yang Z 2015 *Phys. Rev. B* **92**(16) 165418
[90] Zhang J, Zhao B, Zhou T, Xue Y, Ma C and Yang Z 2018 *Phys. Rev. B* **97** 085401 URL https://link.aps.org/doi/10.1103/PhysRevB.97.085401
[91] Farooq M U and Hong J 2019 *npj 2D Materials and Applications* **3** 1–7
[92] Cardoso C, Soriano D, García-Martínez N A and Fernández-Rossier J 2018 *Phys. Rev. Lett.* **121**(6) 067701 URL https://link.aps.org/doi/10.1103/PhysRevLett.121.067701
[93] Seyler K L, Zhong D, Huang B, Linpeng X, Wilson N P, Taniguchi T, Watanabe K, Yao W, Xiao D, McGuire M A, Fu K M C and Xu X 2018 *Nano Lett.* **18** 3823 URL https://pubs.acs.org/sharingguidelineshttp://pubs.acs.org/doi/10.1021/acs.nanolett.8b01105
[94] Zhang G, Guo F, Wu H, Wen X, Yang L, Jin W, Zhang W and Chang H 2022 *Nature Communications* **13** 5067
[95] Zhang X, Lu Q, Liu W, Niu W, Sun J, Cook J, Vaninger M, Miceli P F, Singh D J, Lian S W *et al.* 2021 *Nature communications* **12** 2492
[96] Wang Z, Tang C, Sachs R, Barlas Y and Shi J 2015 *Phys. Rev. Lett.* **114**(1) 016603
[97] Mendes J B S, Alves Santos O, Meireles L M, Lacerda R G, Vilela-Leão L H, Machado F L A,

Rodríguez-Suárez R L, Azevedo A and Rezende S M 2015 *Phys. Rev. Lett.* **115** 226601 URL https://link.aps.org/doi/10.1103/PhysRevLett.115.226601
[98] Yang B, Bhujel B, Chica D G, Telford E J, Roy X, Cosset-Chéneau M and van Wees B J 2023 *arXiv:2312.07131*
[99] Kaverzin A A, Ghiasi T S, Dismukes A H, Roy X and van Wees B J 2022 *2D Materials* **9** 045003 URL https://dx.doi.org/10.1088/2053-1583/ac7881
[100] Heersche H B, Jarillo-Herrero P, Oostinga J B, Vandersypen L M and Morpurgo A F 2007 *Nature* **446** 56–59
[101] Calado V E, Goswami S, Nanda G, Diez M, Akhmerov A R, Watanabe K, Taniguchi T, Klapwijk T M and Vandersypen L M 2015 *Nature nanotechnology* **10** 761–764
[102] Amet F, Ke C T, Borzenets I V, Wang J, Watanabe K, Taniguchi T, Deacon R S, Yamamoto M, Bomze Y, Tarucha S *et al.* 2016 *Science* **352** 966–969
[103] Moriya R, Yabuki N and Machida T 2020 *Phys. Rev. B* **101**(5) 054503 URL https://link.aps.org/doi/10.1103/PhysRevB.101.054503
[104] Gani Y S, Steinberg H and Rossi E 2019 *Phys. Rev. B* **99**(23) 235404 URL https://link.aps.org/doi/10.1103/PhysRevB.99.235404
[105] Naimer T, Gmitra M and Fabian J 2024 *arXiv:2402.07533*
[106] Zhang Z, Watanabe K, Taniguchi T and LeRoy B J 2020 *Phys. Rev. B* **102**(8) 085429 URL https://link.aps.org/doi/10.1103/PhysRevB.102.085429
[107] Högl P, Frank T, Kochan D, Gmitra M and Fabian J 2020 *Phys. Rev. B* **101**(24) 245441 URL https://link.aps.org/doi/10.1103/PhysRevB.101.245441
[108] Gmitra M and Fabian J 2017 *Phys. Rev. Lett.* **119**(14) 146401
[109] Zollner K, Gmitra M and Fabian J 2018 *New J. Phys.* **20** 073007
[110] Perkins D T S and Ferreira A 2024 *Phys. Rev. B* **109**(4) L041411 URL https://link.aps.org/doi/10.1103/PhysRevB.109.L041411
[111] Zhumagulov Y, Kochan D and Fabian J 2023 *arXiv:2307.16025*
[112] Szalowski K, Milivojevic M, Kochan D and gmitra m 2023 *2D Materials* URL http://iopscience.iop.org/article/10.1088/2053-1583/acbb19
[113] Li J, Li Y, Du S, Wang Z, Gu B L, Zhang S C, He K, Duan W and Xu Y 2019 *Science Advances* **5** eaaw5685 URL https://www.science.org/doi/abs/10.1126/sciadv.aaw5685
[114] Zhang P, Yaji K, Hashimoto T, Ota Y, Kondo T, Okazaki K, Wang Z, Wen J, Gu G D, Ding H and Shin S 2018 *Science* **360** 182–186 URL https://www.science.org/doi/abs/10.1126/science.aan4596
[115] Bonilla M, Kolekar S, Ma Y, Diaz H C, Kalappattil V, Das R, Eggers T, Gutierrez H R, Phan M H and Batzill M 2018 *Nat. Nanotechnol.* **13** 289
[116] Shen C, Chu Y, Wu Q, Li N, Wang S, Zhao Y, Tang J, Liu J, Tian J, Watanabe K *et al.* 2020 *Nature Physics* **16** 520–525
[117] Chen S, He M, Zhang Y H, Hsieh V, Fei Z, Watanabe K, Taniguchi T, Cobden D H, Xu X, Dean C R *et al.* 2021 *Nature Physics* **17** 374–380
[118] Park J M, Cao Y, Watanabe K, Taniguchi T and Jarillo-Herrero P 2021 *Nature* **590** 249–255
[119] Crépieux A, Pangburn E, Haurie L, Awoga O A, Black-Schaffer A M, Sedlmayr N, Pépin C and Bena C 2023 *Phys. Rev. B* **108**(13) 134515 URL https://link.aps.org/doi/10.1103/PhysRevB.108.134515
[120] Zhumagulov Y, Frank T and Fabian J 2022 *Phys. Rev. B* **105**(20) 205134 URL https://link.aps.org/doi/10.1103/PhysRevB.105.205134
[121] Kane C L and Mele E J 2005 *Phys. Rev. Lett.* **95** 146802
[122] Qiao Z, Yang S A, Feng W, Tse W K, Ding J, Yao Y, Wang J and Niu Q 2010 *Phys. Rev. B* **82**(16) 161414 URL https://link.aps.org/doi/10.1103/PhysRevB.82.161414
[123] Yang Y, Xu Z, Sheng L, Wang B, Xing D Y and Sheng D N 2011 *Phys. Rev. Lett.* **107**(6) 066602 URL https://link.aps.org/doi/10.1103/PhysRevLett.107.066602
[124] Frank T, Gmitra M and Fabian J 2016 *Phys. Rev. B* **93** 155142
[125] Zollner K, Cummings A W, Roche S and Fabian J 2021 *Phys. Rev. B* **103**(7) 075129
[126] Naimer T, Zollner K, Gmitra M and Fabian J 2021 *Physical Review B* **104** 195156
[127] Young A, Sanchez-Yamagishi J, Hunt B, Choi S, Watanabe K, Taniguchi T, Ashoori R and Jarillo-Herrero P 2014 *Nature* **505** 528–532
[128] Hatsuda K, Mine H, Nakamura T, Li J, Wu R, Katsumoto S and Haruyama J 2018 *Science Advances* **4** eaau6915 URL https://www.science.org/doi/abs/10.1126/sciadv.aau6915
[129] Martin J, Akerman N, Ulbricht G, Lohmann T, Smet J H, von Klitzing K and Yacoby A 2008 *Nat. Phys.* **4** 144
[130] Gibertini M, Tomadin A, Guinea F, Katsnelson M I and Polini M 2012 *Phys. Rev. B* **85**(20) 201405 URL https://link.aps.org/doi/10.1103/PhysRevB.85.201405

[131] Tiwari P, Srivastav S K, Ray S, Das T and Bid A 2020 *ACS Nano* **15** 916–922 ISSN 1936-086X URL http://dx.doi.org/10.1021/acsnano.0c07524

[132] Han T, Lu Z, Yao Y, Yang J, Seo J, Yoon C, Watanabe K, Taniguchi T, Fu L, Zhang F and Ju L 2024 *Science* **384** 647–651 (*Preprint* https://www.science.org/doi/pdf/10.1126/science.adk9749) URL https://www.science.org/doi/abs/10.1126/science.adk9749

[133] Cao Y, Fatemi V, Demir A, Fang S, Tomarken S L, Luo J Y, Sanchez-Yamagishi J D, Watanabe K, Taniguchi T, Kaxiras E, Ashoori R C and Jarillo-Herrero P 2018 *Nature* **556** 80 URL http://dx.doi.org/10.1038/nature26154http://www.nature.com/articles/nature26154

[134] Stepanov P, Das I, Lu X, Fahimniya A, Watanabe K, Taniguchi T, Koppens F H, Lischner J, Levitov L and Efetov D K 2020 *Nature* **583** 375–378

[135] Sharpe A L, Fox E J, Barnard A W, Finney J, Watanabe K, Taniguchi T, Kastner M A and Goldhaber-Gordon D 2019 *Science* **365** 605–608 ISSN 0036-8075

[136] Saito Y, Yang F, Ge J, Liu X, Taniguchi T, Watanabe K, Li J, Berg E and Young A F 2021 *Nature* **592** 220–224

[137] Serlin M, Tschirhart C L, Polshyn H, Zhang Y, Zhu J, Watanabe K, Taniguchi T, Balents L and Young A F 2020 *Science* **367** 900–903

[138] Nimbalkar A and Kim H 2020 *Nano-Micro Letters* **12** 126

[139] Bultinck N, Chatterjee S and Zaletel M P 2020 *Phys. Rev. Lett.* **124**(16) 166601

[140] Repellin C, Dong Z, Zhang Y H and Senthil T 2020 *Phys. Rev. Lett.* **124**(18) 187601

[141] Choi Y, Kemmer J, Peng Y, Thomson A, Arora H, Polski R, Zhang Y, Ren H, Alicea J, Refael G *et al.* 2019 *Nature Physics* **15** 1174–1180

[142] Lisi S, Lu X, Benschop T, de Jong T A, Stepanov P, Duran J R, Margot F, Cucchi I, Cappelli E, Hunter A *et al.* 2021 *Nature Physics* **17** 189–193

[143] Balents L, Dean C R, Efetov D K and Young A F 2020 *Nature Physics* **16** 725–733

[144] Wolf T M R, Lado J L, Blatter G and Zilberberg O 2019 *Phys. Rev. Lett.* **123**(9) 096802

[145] Carr S, Fang S, Zhu Z and Kaxiras E 2019 *Phys. Rev. Res.* **1**(1) 013001 URL https://link.aps.org/doi/10.1103/PhysRevResearch.1.013001

[146] Lucignano P, Alfè D, Cataudella V, Ninno D and Cantele G 2019 *Phys. Rev. B* **99**(19) 195419 URL https://link.aps.org/doi/10.1103/PhysRevB.99.195419

[147] Song Z D and Bernevig B A 2022 *Phys. Rev. Lett.* **129**(4) 047601 URL https://link.aps.org/doi/10.1103/PhysRevLett.129.047601

[148] Koh J M, Alicea J and Lantagne-Hurtubise E 2024 *Phys. Rev. B* **109**(3) 035113 URL https://link.aps.org/doi/10.1103/PhysRevB.109.035113

[149] Han T, Lu Z, Yao Y, Yang J, Seo J, Yoon C, Watanabe K, Taniguchi T, Fu L, Zhang F and Ju L 2024 *Science* **384** 647–651 (*Preprint* https://www.science.org/doi/pdf/10.1126/science.adk9749) URL https://www.science.org/doi/abs/10.1126/science.adk9749

[150] Zhu Z, Carr S, Massatt D, Luskin M and Kaxiras E 2020 *Phys. Rev. Lett.* **125**(11) 116404

[151] Chou Y Z, Wu F, Sau J D and Das Sarma S 2021 *Phys. Rev. Lett.* **127**(18) 187001 URL https://link.aps.org/doi/10.1103/PhysRevLett.127.187001

[152] Park J M, Cao Y, Xia L, Sun S, Watanabe K, Taniguchi T and Jarillo-Herrero P 2021 *arXiv:2112.10760*

[153] Su R, Kuiri M, Watanabe K, Taniguchi T and Folk J 2023 *Nature Materials* **22** 1332–1337

[154] Curtis J B, Poniatowski N R, Xie Y, Yacoby A, Demler E and Narang P 2023 *Phys. Rev. Lett.* **130**(19) 196001 URL https://link.aps.org/doi/10.1103/PhysRevLett.130.196001

[155] Jimeno-Pozo A, Sainz-Cruz H, Cea T, Pantaleón P A and Guinea F 2023 *Phys. Rev. B* **107**(16) L161106 URL https://link.aps.org/doi/10.1103/PhysRevB.107.L161106

[156] Holleis L, Patterson C L, Zhang Y, Vituri Y, Yoo H M, Zhou H, Taniguchi T, Watanabe K, Berg E, Nadj-Perge S and Young A F 2024 *arXiv:2303.00742* URL https://arxiv.org/abs/2303.00742

[157] Piquemal-Banci M, Galceran R, Dubois S M M, Zatko V, Galbiati M, Godel F, Martin M B, Weatherup R S, Petroff F, Fert A *et al.* 2020 *Nature Communications* **11** 5670

[158] Piquemal-Banci M, Galceran R, Martin M B, Godel F, Anane A, Petroff F, Dlubak B and Seneor P 2017 *Journal of Physics D: Applied Physics* **50** 203002 URL https://dx.doi.org/10.1088/1361-6463/aa650f

[159] Avsar A, Unuchek D, Liu J, Sanchez O L, Watanabe K, Taniguchi T, Özyilmaz B and Kis A 2017 *ACS Nano* **11** 11678

[160] Luo Y K, Xu J, Zhu T, Wu G, McCormick E J, Zhan W, Neupane M R and Kawakami R K 2017 *Nano Lett.* **17** 3877

[161] Khokhriakov D, Sayed S, Hoque A M, Karpiak B, Zhao B, Datta S and Dash S P 2022 *Phys. Rev. Appl.* **18**(6) 064063 URL https://link.aps.org/doi/10.1103/PhysRevApplied.18.064063

[162] Pandey L, Zhao B, Ngaloy R, Bangar H, Ali A, Abdel-Hafiez M, Zhang G, Wu H, Chang H, Sjöström L *et al.* 2024 *arXiv preprint arXiv:2408.13095*
[163] Dolui K, Petrovic M D, Zollner K, Plechac P, Fabian J and Nikolic B K 2020 *Nano letters* **20** 2288–2295
[164] Zhao B, Bainsla L, Ngaloy R, Svedlindh P and Dash S P 2023 *arXiv preprint arXiv:2308.13408*
[165] Kajale S N, Nguyen T, Hung N T, Li M and Sarkar D 2024 *Science advances* **10** eadk8669
[166] Li W, Zhu W, Zhang G, Wu H, Zhu S, Li R, Zhang E, Zhang X, Deng Y, Zhang J *et al.* 2023 *Advanced Materials* **35** 2303688
[167] Guillet T, Galceran R, Sierra J F, Belarre F J, Ballesteros B, Costache M V, Dosenovic D, Okuno H, Marty A, Jamet M *et al.* 2024 *Nano Letters* **24** 822–828
[168] Yang B, Patel T, Cheng M, Pichugin K, Tian L, Sherlekar N, Yan S, Fu Y, Tian S, Lei H *et al.* 2024 *Nature Communications* **15** 4982
[169] Chen Y, Samanta K, Shahed N A, Zhang H, Fang C, Ernst A, Tsymbal E Y and Parkin S S 2024 *Nature* **632** 1045–1051